

Original articles

Computational analysis of the conserved curvature driven flow for open curves in the plane

Miroslav Kolář^{a,*}, Michal Beneš^a, Daniel Ševčovič^b^a Department of Mathematics, Faculty of Nuclear Sciences and Physical Engineering, Czech Technical University in Prague, Trojanova 13, 120 00, Prague 2, Czech Republic^b Department of Applied Mathematics and Statistics, Faculty of Mathematics, Physics and Informatics, Comenius University, 842 48, Bratislava, Slovakia

Received 6 May 2015; accepted 13 February 2016

Available online 7 March 2016

Abstract

The paper studies the constrained curvature flow for open planar curves with fixed endpoints by means of its numerical solution. This law originates in the theory of phase transitions for crystalline materials and where it describes the evolution of closed embedded curves with constant enclosed area. We show that the area is preserved for open curves with fixed endpoints as well. Here, the area is given by the curve and its ends connected to the origin of coordinates. We provide the form of the stationary solution towards which any other solution converges asymptotically in time. The evolution law is reformulated by means of the direct method into the system of degenerate parabolic partial differential equations for the curve parametrization. This system is spatially discretized by means of the flowing finite volumes method and solved numerically by the explicit Runge–Kutta solver. We experimentally investigate the order of approximation of the scheme by means of our numerical data and by knowing the analytical solution. We also discuss the role of the suitable tangential redistribution. For this purpose, several computational studies related to the open curve dynamics are presented.

© 2016 International Association for Mathematics and Computers in Simulation (IMACS). Published by Elsevier B.V. All rights reserved.

Keywords: Phase transitions; Area-preserving curvature flow; Parametric method; Open curves; Experimental order of convergence

1. Introduction

In this article we focus on the non-local curvature flow for open curves in \mathbb{R}^2 . Our main goal is to investigate the flow described by the following geometric evolution law:

$$v_\Gamma = -\kappa_\Gamma + F, \quad \text{where } F = \frac{1}{L(\Gamma_t)} \int_{\Gamma_t} \kappa_\Gamma ds, \quad (1)$$

$$\Gamma_t|_{t=0} = \Gamma_{ini}, \quad (2)$$

* Corresponding author.

E-mail addresses: kolarmir@fjfi.cvut.cz (M. Kolář), michal.benes@fjfi.cvut.cz (M. Beneš), sevcovic@fmph.uniba.sk (D. Ševčovič).

where Γ_t is a C^1 smooth open curve with fixed endpoints in \mathbb{R}^2 . It is evolved in the normal direction with the velocity v_Γ . The evolution starts from the initial curve Γ_{ini} . Here $L(\Gamma_t) = \int_{\Gamma_t} ds$ is the length of the curve Γ_t and κ_Γ is the (mean) curvature of Γ_t .

In the case where Γ_t is a closed Jordan curve, \mathbf{n}_Γ is the outward unit normal vector and the curve is assumed to be oriented counter-clockwise. This means, that $\kappa_\Gamma = 1$ if Γ_t is the unit circle. In the other cases, i.e., the case where Γ_t is an open curve or a self-intersected closed curve, \mathbf{n}_Γ is chosen in such a way that $\det(\mathbf{n}_\Gamma, \mathbf{t}_\Gamma) = 1$ where \mathbf{t}_Γ is the unit tangent vector to the Γ_t (see Section 2).

Geometric laws similar to (1) have been discussed in the literature (see [14,11,20,13]) or [18]. They belong to a class of (mean) curvature flows described by the evolution law

$$v_\Gamma = -\kappa_\Gamma + F, \quad (3)$$

with a particular choice of the forcing term F , which is widely studied in the literature (see, e.g., [12]) The evolution of open curves has been addressed, e.g., in [5,22] or in [23].

The global character of the forcing term F often plays its role in the constrained motion by (mean) curvature, where the F depends on geometrical properties of Γ_t , like its length $L(\Gamma_t)$, enclosed area $A(\Gamma_t)$ etc. The particular choice of F as in (1), i.e., $F = \int_{\Gamma_t} \kappa_\Gamma ds / L(\Gamma_t)$, leads to the area preserving (mean) curvature flow, whereas $F = \int_{\Gamma_t} \kappa_\Gamma^2 ds / \int_{\Gamma_t} \kappa_\Gamma ds$ yields the length preserving (mean) curvature flow (see [30]), or, by choosing the force as $F = L(\Gamma_t) / 2A(\Gamma_t)$, we can investigate the isoperimetric ratio gradient flow (see [30]).

The local character of F is often observed in applications of the (mean) curvature flow in digital image processing. Namely in image segmentation, where the force F locally depends on the intensity of the segmented image (see, e.g., [3,4]).

The (mean) curvature flow with a particular choice of the forcing term F found its applications in many problems with physical context, e.g., in dislocation dynamics in crystalline materials, where F can describe either global stress field or local interaction forces between multiple defects (see [6,22]). The constrained motion by (mean) curvature, in particular, has been investigated in [27,17,7] within the context of a modification of the Allen–Cahn equation (see [8,1]) approximating the (mean) curvature flow (see [2]). The non-local character of the geometric governing equation is also connected to the recrystallization phenomena where a fixed previously melted volume of the liquid phase solidifies again (see [19]).

Problem (3) for closed curves can be mathematically treated by the direct (parametric) method (see, e.g., [10,12,4]), by the level set method (see, e.g., [24]) or by the phase-field method (see, e.g., [2]). In this paper, we investigate (3) by means of the direct method as the single option for open or self-intersecting curves and solve the resulting degenerate parabolic system numerically to provide the information on the solution behavior. For this purpose, the used numerical scheme based on the flowing finite volume method is suggested using the previous authors' experience. Approximation property of this scheme is analyzed and the role of the redistribution for its stable behavior is explained. Then, several computational examples are presented.

2. Equations

In the direct method for solving (1) one considers the parametrization of the smooth time-dependent curve Γ_t for $t \geq 0$ by means of the mapping

$$\vec{X} = \vec{X}(t, u), \quad u \in [0, 1],$$

where u is the parameter in a fixed interval. In the case of a closed curve, the parametrization is orientated counter-clockwise and the periodic boundary conditions at $u = 0$ and $u = 1$ are imposed, i.e. $\vec{X}(t, 0) = \vec{X}(t, 1)$. For open curves with fixed ends we prescribe the Dirichlet boundary conditions for $\vec{X}(t, u)$ at $u = 0$ and $u = 1$; i.e. $\vec{X}(t, 0) = \vec{X}_0$ and $\vec{X}(t, 1) = \vec{X}_1$ for given positions \vec{X}_0 and \vec{X}_1 , respectively. Consequently, the geometric quantities of our interest can be expressed by means of the mapping \vec{X} . The unit tangent and normal vectors are given by the following formulas:

$$\mathbf{t}_\Gamma = \frac{\partial_u \vec{X}}{|\partial_u \vec{X}|} \quad \text{and} \quad \mathbf{n}_\Gamma = \frac{\partial_u \vec{X}^\perp}{|\partial_u \vec{X}|} = \frac{1}{|\partial_u \vec{X}|} \begin{pmatrix} \partial_u X^2 \\ -\partial_u X^1 \end{pmatrix}, \quad \text{where } \vec{X} = \begin{pmatrix} X^1 \\ X^2 \end{pmatrix}$$

in accordance with the rule $\det(\mathbf{n}_\Gamma, \mathbf{t}_\Gamma) = 1$. For the (mean) curvature κ_Γ we have

$$\kappa_\Gamma(\vec{X}) = -\frac{1}{|\partial_u \vec{X}|} \partial_u \left(\frac{\partial_u \vec{X}}{|\partial_u \vec{X}|} \right) \cdot \mathbf{n}_\Gamma, \tag{4}$$

and the normal velocity in the direction of \mathbf{n}_Γ (the projection of the point velocity \vec{v}_Γ at Γ to \mathbf{n}_Γ) becomes

$$v_\Gamma = \vec{v}_\Gamma \cdot \mathbf{n}_\Gamma \quad \text{where } \vec{v}_\Gamma = \partial_t \vec{X}.$$

The curve Γ_t evolves according to (1), provided $\vec{X} = \vec{X}(t, u)$ satisfies the following system

$$\partial_t \vec{X} = \frac{1}{|\partial_u \vec{X}|} \partial_u \left(\frac{\partial_u \vec{X}}{|\partial_u \vec{X}|} \right) + F \frac{\partial_u \vec{X}^\perp}{|\partial_u \vec{X}|} \quad \text{in } (0, T) \times (0, 1), \tag{5}$$

$$\vec{X}|_{t=0} = \vec{X}|_{\text{ini}}, \tag{6}$$

where in the case of flow (1) with nonlocally defined forcing term we have

$$F = \int_{\Gamma_t} \kappa_\Gamma ds / L(\Gamma_t), \tag{7}$$

$$L(\Gamma_t) = \int_{\Gamma_t} ds = \int_0^1 |\partial_u \vec{X}| du, \quad \int_{\Gamma_t} \kappa_\Gamma ds = \int_0^1 \kappa_\Gamma(\vec{X}) |\partial_u \vec{X}| du.$$

This is known as the parametric (direct) description of (1).

The details on the general motion law (3) treated by this approach can be found, e.g., in [28], in [10,9] or in [22]. Among advantages of this approach, an easy and straightforward numerical treatment of the curve dynamics is offered. On the other hand, topological changes can not be treated straightforwardly although there are recent algorithms for handling topological changes (see, e.g., [4,25,26]).

Denoting

$$A(\Gamma_t) = \frac{1}{2} \int_0^1 \det(\vec{X}, \partial_u \vec{X}) du, \tag{8}$$

the flow governed by (1) preserves $A = A(\Gamma_t)$, i.e. $A(\Gamma_t) = A(\Gamma_{\text{ini}})$ for all $t \geq 0$. In the case where Γ_t is the Jordan curve, the quantity A represents the enclosed area $A(\Gamma_t)$. And in the case where Γ_t is an open curve with fixed ends the quantity A represents the area enclosed by the curve Γ_t and lines connecting the fixed ends with the origin of the coordinates (see Fig. 2). The following result is known for the case when Γ_t is the Jordan curve (see, e.g., [29]). We extend it for the case when Γ_t is the open curve with fixed endpoints.

Proposition 1. *Suppose $\{\Gamma_t\}_{t \geq 0}$ is a family of C^1 smooth planar curves, evolving in the normal direction according to (5)–(6). If Γ_t are either closed, or open curves with the fixed endpoints, then*

$$\frac{dA(\Gamma_t)}{dt} = \int_{\Gamma_t} v_\Gamma ds. \tag{9}$$

In particular, for each v_Γ in the form

$$v_\Gamma = f - \frac{1}{L(\Gamma_t)} \int_{\Gamma_t} f ds,$$

where f is a smooth function defined on Γ_t we obtain that

$$\frac{dA(\Gamma_t)}{dt} = 0. \tag{10}$$

Proof. Differentiating (8) we obtain

$$\begin{aligned}
 \frac{dA(\Gamma_t)}{dt} &= \frac{1}{2} \frac{d}{dt} \int_0^1 \det(\vec{X}, \partial_u \vec{X}) du \\
 &= \frac{1}{2} \int_0^1 \det(\partial_t \vec{X}, \partial_u \vec{X}) du + \frac{1}{2} \int_0^1 \det(\vec{X}, \partial_{tu}^2 \vec{X}) du \\
 &= \int_0^1 \det(\partial_t \vec{X}, \partial_u \vec{X}) du + \frac{1}{2} \int_0^1 \partial_u \det(\vec{X}, \partial_t \vec{X}) du \\
 &= \int_{\Gamma_t} v_\Gamma ds + \frac{1}{2} \left[\det(\vec{X}, \partial_t \vec{X}) \right]_0^1
 \end{aligned} \tag{11}$$

Eq. (3) is valid provided the mapping \vec{X} satisfies the following

$$\partial_t \vec{X} = (-\kappa_\Gamma + F) \mathbf{n}_\Gamma.$$

From the latter integral expression we deduce

$$\frac{dA(\Gamma_t)}{dt} = \int_{\Gamma_t} v_\Gamma ds + \frac{1}{2} \left[\det(\vec{X}, \partial_t \vec{X}) \right]_0^1.$$

The following identity

$$\left[\det(\vec{X}, \partial_t \vec{X}) \right]_0^1 = 0$$

is valid provided that either Γ_t is a closed curve ($\vec{X}(t, 0) = \vec{X}(t, 1)$) or Γ_t is an open curve with the fixed endpoints ($\partial_t \vec{X}(t, 0) = \partial_t \vec{X}(t, 1) = 0$). Moreover, if the normal velocity has the form $v_\Gamma = f - \frac{1}{L(\Gamma_t)} \int_{\Gamma_t} f ds$, then $\int_{\Gamma_t} v_\Gamma ds$ vanishes since $\int_{\Gamma_t} ds = L(\Gamma_t)$. Then

$$\frac{dA(\Gamma_t)}{dt} = 0$$

holds for any sufficiently smooth function f .

Remark 1. It follows that (10) holds for the choice of $f = \kappa_\Gamma$ in agreement with (7).

Remark 2. The asymptotic behavior of curves evolving according to (3) has been studied mainly by [16,15]. They assumed $F = 0$, and proved that any smooth closed convex curve embedded in \mathbb{R}^2 evolved by the curvature converges to a point in finite time with asymptotic circular shape (see [15]). Furthermore, any smooth closed curve embedded in \mathbb{R}^2 evolved by the curvature becomes convex in finite time and then it converges to a point in finite time with asymptotic circular shape (see [16]). In the case of law (1), the closed simple curve asymptotically achieves circular shape enclosing the same area, as discussed, e.g., by [27,18,7,30]. For the open non-intersecting curves connecting fixed ends one can hypothesize that the curve asymptotically attains the shape corresponding to the arc (the part of circle) with radius given by the initial area obtained by connecting the curve with the origin of coordinates — see Figs. 2 and 3. In this article, we present the computational results which comply with this hypothesis.

Tangential effects

Further modifications of (3) lead to the form of law (5) with tangential terms proposed, e.g., in [12] for closed curves and applied by [6]. Instead of (5), one can consider the evolution law

$$\partial_t \vec{X} = \frac{1}{|\partial_u \vec{X}|} \partial_u \left(\frac{\partial_u \vec{X}}{|\partial_u \vec{X}|} \right) + F \frac{\partial_u \vec{X}^\perp}{|\partial_u \vec{X}|} + \alpha_{loc} \frac{\partial_u \vec{X}}{|\partial_u \vec{X}|} \quad \text{in } (0, T) \times [0, 1], \tag{12}$$

where, according to [21], the local tangential velocity α_{loc}

$$\alpha_{loc} = -\partial_u \left(\frac{1}{|\partial_u \vec{X}|} \right) = \frac{\partial_u \vec{X} \cdot \partial_{uu} \vec{X}}{|\partial_u \vec{X}|^3}.$$

Law (12) then becomes

$$\partial_t \vec{X} = \frac{\partial_{uu} \vec{X}}{|\partial_u \vec{X}|^2} + F \frac{\partial_u \vec{X}^\perp}{|\partial_u \vec{X}|} \quad \text{in } (0, T) \times [0, 1]. \tag{13}$$

It contains a nontrivial locally defined tangential velocity. Unlike (5), the modified system (12) contains the local tangential term $\alpha_{loc} \mathbf{t}_\Gamma$. However, numerical experiments often show this local tangential redistribution is not enough to provide satisfactory results on its own. Therefore, it is useful to replace it by a general tangential velocity denoted by α , such that

$$\partial_t \vec{X} = \frac{1}{|\partial_u \vec{X}|} \partial_u \left(\frac{\partial_u \vec{X}}{|\partial_u \vec{X}|} \right) + F \frac{\partial_u \vec{X}^\perp}{|\partial_u \vec{X}|} + \alpha \frac{\partial_u \vec{X}}{|\partial_u \vec{X}|} \quad \text{in } (0, T) \times [0, 1]. \tag{14}$$

Here α is a general, possibly nonlocally defined tangential velocity. There are various ways how to choose the tangential velocity α . For a discussion on the choice of α we refer to [21]. If properly chosen, the numerical algorithm is more stable and shows better accuracy. Notice that the tangential velocity does not change the shape of the evolved curves in case either Γ_t is closed or Γ_t is an open curve with the fixed ends provided α vanishes at the endpoints, i.e. $\alpha|_{u=0} = \alpha|_{u=1} = 0$. For example, if α satisfies

$$\frac{1}{|\partial_u \vec{X}|} \partial_u \alpha = \kappa_\Gamma v_\Gamma - \langle \kappa_\Gamma v_\Gamma \rangle_\Gamma + \omega \left(\frac{L(\Gamma_t)}{|\partial_u \vec{X}|} - 1 \right), \tag{15}$$

where $\alpha|_{u=0} = 0$ and $\langle f \rangle_\Gamma = \frac{1}{L(\Gamma_t)} \int_{\Gamma_t} f ds$ is the curve average of the quantity f , then tangential redistribution α vanishes at the other endpoint $\alpha|_{u=1} = 0$ as well, ω is a given scalar parameter.

3. Numerical solution

For the space discretization of (14), the method of flowing finite volumes is used as, e.g., in [22]. The discrete nodes $\mathbf{X}_i = \mathbf{X}(t, u_i)$, $i = 0, \dots, M$, as well as dual nodes $\mathbf{X}_{i\pm\frac{1}{2}} = \mathbf{X}(t, u_{i\pm\frac{1}{2}})$ for $u_{i\pm\frac{1}{2}} = u_i \pm h/2$, $i = 1, \dots, M$, $h = 1/M$, are positioned along Γ_t as shown in Fig. 1. Notice that $(\mathbf{X}_i + \mathbf{X}_{i\pm 1})/2$ denote averages on segments connecting nearby discrete nodes and differs from $\mathbf{X}_{i\pm\frac{1}{2}} \in \Gamma_t$. The governing equation is integrated along the dual segments surrounding the nodes \mathbf{X}_i , $i = 1, \dots, M - 1$ resulting into

$$\begin{aligned} \int_{u_{i-\frac{1}{2}}}^{u_{i+\frac{1}{2}}} \partial_t \mathbf{X} |\partial_u \mathbf{X}| du &= \int_{u_{i-\frac{1}{2}}}^{u_{i+\frac{1}{2}}} \partial_u \left(\frac{\partial_u \mathbf{X}}{|\partial_u \mathbf{X}|} \right) du + F \int_{u_{i-\frac{1}{2}}}^{u_{i+\frac{1}{2}}} \partial_u \mathbf{X}^\perp du + \int_{u_{i-\frac{1}{2}}}^{u_{i+\frac{1}{2}}} \alpha \partial_u \vec{X} du, \\ F &= \frac{1}{\int_0^1 |\partial_u \mathbf{X}| du} \int_0^1 \kappa_\Gamma |\partial_u \mathbf{X}| du, \\ \kappa_\Gamma &= -\frac{1}{|\partial_u \mathbf{X}|} \partial_u \left(\frac{\partial_u \mathbf{X}}{|\partial_u \mathbf{X}|} \right) \cdot \frac{\partial_u \mathbf{X}^\perp}{|\partial_u \mathbf{X}|}. \end{aligned} \tag{16}$$

Evaluating the first integral on the right-hand side, we obtain

$$\int_{u_{i-\frac{1}{2}}}^{u_{i+\frac{1}{2}}} \partial_t \mathbf{X} |\partial_u \mathbf{X}| du = \left. \frac{\partial_u \mathbf{X}}{|\partial_u \mathbf{X}|} \right|_{u_{i+\frac{1}{2}}} - \left. \frac{\partial_u \mathbf{X}}{|\partial_u \mathbf{X}|} \right|_{u_{i-\frac{1}{2}}} + F \int_{u_{i-\frac{1}{2}}}^{u_{i+\frac{1}{2}}} \partial_u \mathbf{X}^\perp du + \int_{u_{i-\frac{1}{2}}}^{u_{i+\frac{1}{2}}} \alpha \partial_u \vec{X} du. \tag{17}$$

We denote the discrete quantities

$$d_j = |\mathbf{X}_j - \mathbf{X}_{j-1}| \quad \text{for } j = 1, \dots, M,$$

where $\mathbf{X}_0 = \mathbf{X}_M$ and $\mathbf{X}_{M+1} = \mathbf{X}_1$ for closed Γ_t , or $\mathbf{X}_0, \mathbf{X}_M$ fixed for open Γ_t , and

$$\kappa_i = -\frac{2}{d_i + d_{i+1}} \left(\frac{\mathbf{X}_{i+1} - \mathbf{X}_i}{d_{i+1}} - \frac{\mathbf{X}_i - \mathbf{X}_{i-1}}{d_i} \right) \cdot \frac{\mathbf{X}_{i+1}^\perp - \mathbf{X}_{i-1}^\perp}{d_i + d_{i+1}}.$$

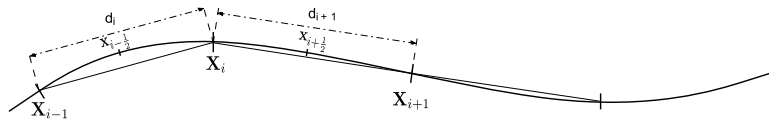
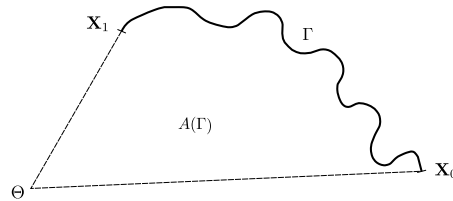


Fig. 1. Curve discretization by finite volumes.

Fig. 2. Area enclosed by the curve Γ_t and the lines connecting the origin Θ of coordinates.

Considering the approximation of the integrals by the finite-volume method along the curve, we have

$$\int_{u_{i-\frac{1}{2}}}^{u_{i+\frac{1}{2}}} \partial_t \mathbf{X} |\partial_u \mathbf{X}| du \approx \frac{d\mathbf{X}_i}{dt} \frac{d_i + d_{i+1}}{2}$$

$$\int_{u_{i-\frac{1}{2}}}^{u_{i+\frac{1}{2}}} \partial_u \mathbf{X}^\perp du \approx \frac{(\mathbf{X}_{i+1}^\perp - \mathbf{X}_{i-1}^\perp)}{2}, \quad \int_{u_{i-\frac{1}{2}}}^{u_{i+\frac{1}{2}}} \alpha \partial_u \vec{X} du \approx \alpha_i \frac{(\mathbf{X}_{i+1} - \mathbf{X}_{i-1})}{2}.$$

Discrete approximation of tangential velocity α_i follows from (15) and denotes the value $\alpha_i = \alpha(t, u_i)$. Integration yields the following recurrent formulas

$$\alpha_i = \alpha_1 + \Psi_i, \quad i = 2, \dots, M-1, \quad (18)$$

$$\alpha_1 = -\frac{\sum_{l=2}^M (d_l + d_{l+1}) \Psi_l / 2}{\sum_{l=1}^M (d_l + d_{l+1}) / 2}, \quad (19)$$

$$\Psi_i = \sum_{k=2}^i \psi_k, \quad (20)$$

$$\psi_k = \kappa_k (-\kappa_k + F) d_k - \frac{\sum_{l=1}^M \kappa_l (-\kappa_l + F) d_l}{\sum_{l=1}^M d_l} + \omega \left(\frac{\sum_{l=1}^M d_l}{M} - d_k \right), \quad (21)$$

where we set $\alpha_0 = \alpha_M = 0$. For more detailed analysis of the discretization of the tangential velocity α we refer the reader to, e.g., [21,30]. Finally, the semi-discrete scheme solving (14) within the context of (1) is the following

$$\frac{d\mathbf{X}_i}{dt} \frac{d_i + d_{i+1}}{2} = \left(\frac{\mathbf{X}_{i+1} - \mathbf{X}_i}{d_{i+1}} - \frac{\mathbf{X}_i - \mathbf{X}_{i-1}}{d_i} \right) + F \frac{(\mathbf{X}_{i+1}^\perp - \mathbf{X}_{i-1}^\perp)}{2} + \alpha_i \frac{(\mathbf{X}_{i+1} - \mathbf{X}_{i-1})}{2}, \quad (22)$$

$$F = \frac{1}{\sum_{l=1}^M d_l} \sum_{l=1}^M \kappa_l \frac{d_{l+1} + d_l}{2}, \quad (23)$$

$$\vec{X}_i(0) = \vec{X}_{ini}(u_i), \quad (24)$$

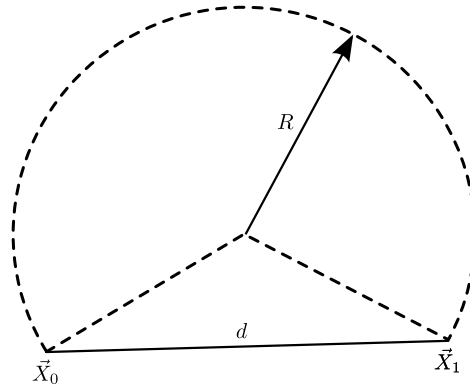


Fig. 3. Schematic figure of the test curve with known area.

for $i = 1, \dots, M - 1$. This system can be solved by means of the 4th-order explicit Runge–Kutta–Merson scheme as in [6], with the automatic time step control and the tolerance parameter $\varepsilon = 10^{-6}$. The initial time step is chosen as h^2 , where $h = 1/M$ is the mesh size dividing the parameter range $[0, 1]$.

Remark 3. Assuming that the solution of (14) with forcing term given by (7) is sufficiently smooth, results of our numerical experiments indicate that finite-volume scheme (22) has the order of integral approximation $\mathcal{O}(h^2)$, where $h = \frac{1}{M}$. In this paper, our main focus lies in computational aspects of constrained motion of open planar curves exhibiting zero tangential velocity on their ends. Detailed discussion on consistency, stability, and convergence of the described numerical scheme together with more general choice of normal velocity will be the subject of our future work.

4. Computational studies

We use scheme (22)–(23) with the tangential redistribution to perform a series of computational studies showing the behavior of solutions to (1).

The following examples demonstrate how a solution of (1) evolves in time approaching the arc shape, which is the asymptotic profile in the case of open curve with fixed ends. The arc is the part of the circle in steady state with the radius R given implicitly by the following equation

$$A(\Gamma_{ini}) = \pi R^2 \left(1 - \frac{1}{\pi} \arcsin \left(\frac{d}{2R} \right) \right),$$

where d is a distance between the fixed ends. This case is illustrated in Fig. 3.

Additionally, the experimental orders of convergence (EoC) have been measured for all testing examples. As the testing parameter for estimation of the order of convergence of our scheme we chose the quantity A representing the enclosed area. We measured the error given by the difference between area at the initial time ($t = 0$) which has been evaluated analytically, and the area at given data output times T_1, T_2, \dots, T_N , where we denote $\Delta t_i = T_i - T_{i-1}, i = 1, 2, \dots, N$. The difference between the analytically given area $A(\Gamma_{ini})$ and the actual area $A(T_i)$ of polygonal domain enclosed by piece-wise linear approximation of Γ_t obtained by (22)–(24) at the time level T_i for given mesh with M elements is evaluated both by the maximum norm as

$$error_1(M) = \max_{i=1,2,\dots,N} |A(\Gamma_{ini}) - A(T_i)|$$

and by the L_1 norm as

$$error_2(M) = \frac{1}{T_N} \sum_{k=1}^N |A(\Gamma_{ini}) - A(T_k)| \Delta t_k \approx \frac{1}{T} \int_0^T |A(\Gamma_{ini}) - A(t)| dt.$$

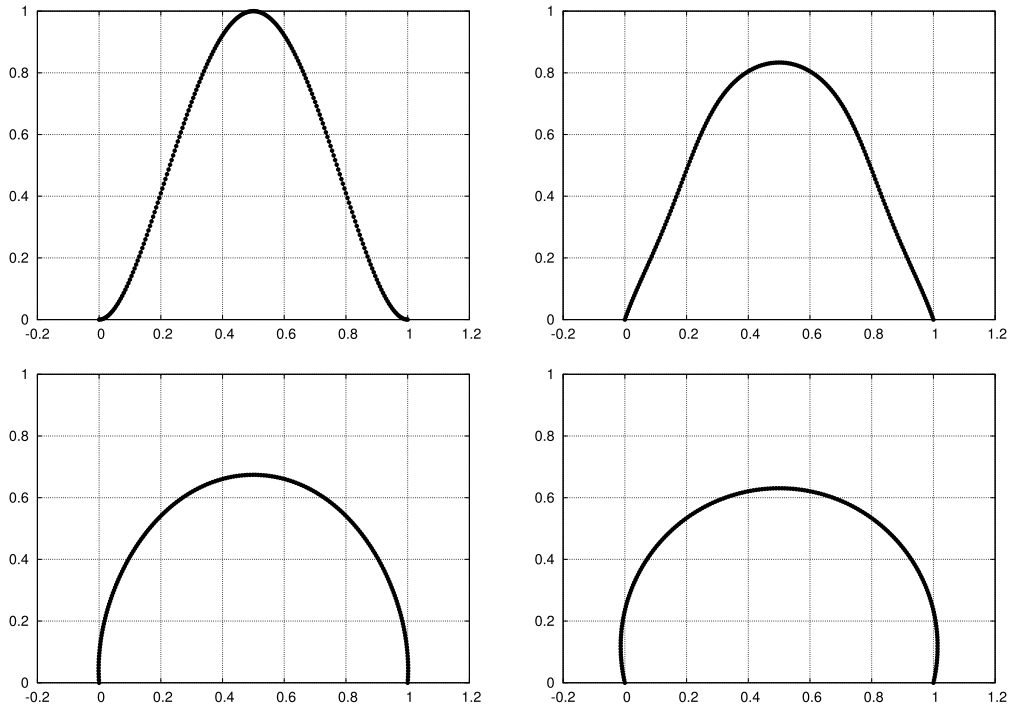


Fig. 4. The area-preserving (mean) curvature flow (1) from Example 1, where the initial open curve asymptotically approaches the arc shape. The curve Γ_t is depicted for $t = 0$, $t = 0.025$, $t = 0.1$ and $t = 0.5$.

Both errors depend on the parameter M , which is the number of finite volumes. Assuming as in [2] and in references therein that both error estimates depend on the number of finite volumes as

$$\text{error}_i(M) = \text{const} \left(\frac{1}{M} \right)^{EoC}, \quad i = 1, 2,$$

we can estimate the order of convergence EoC of scheme (22) between two levels of meshes M_1 and M_2 as

$$EoC = \frac{\log \left(\frac{\text{error}_i(M_1)}{\text{error}_i(M_2)} \right)}{\log \left(\frac{M_2}{M_1} \right)}, \quad i = 1, 2.$$

Example 1. Fig. 4 illustrates behavior of a solution for the initial open curve given by parametric equations

$$\vec{X}(0, u) = \left(1 - u, (4u(1 - u))^2 \right) \quad (25)$$

for $u \in [0, 1]$, i.e. the initial curve is a graph of the fourth-order polynomial. The motion in the time interval $[0, 0.5]$ is driven by the normal velocity given by (1). The number of finite volumes is $M = 200$. The curve Γ_t asymptotically approaches the arc shape whereas the enclosed area is preserved (see [27]). The initial curve encloses the area of 0.533269 and at $t = 0.5$, the curve encloses the area of 0.53334. Table 1 shows the values of EoC for enclosed area.

Example 2. In Fig. 5, the second example shows the behavior of the solution when the initial open curve is given by parametric equations

$$\vec{X}(0, u) = \left((1 + 0.3 \cos(1.2\pi u)) \cos(\pi u), (1 + 0.3 \cos(12\pi u)) \sin(\pi u) \right) \quad (26)$$

for $u \in [0, 1]$. The motion in the time interval $[0, 2.0]$ is driven by the normal velocity given by (1). The number of finite volumes is $M = 200$. The curve Γ_t asymptotically approaches the arc shape, where the preserved quantity $A(\Gamma_t)$

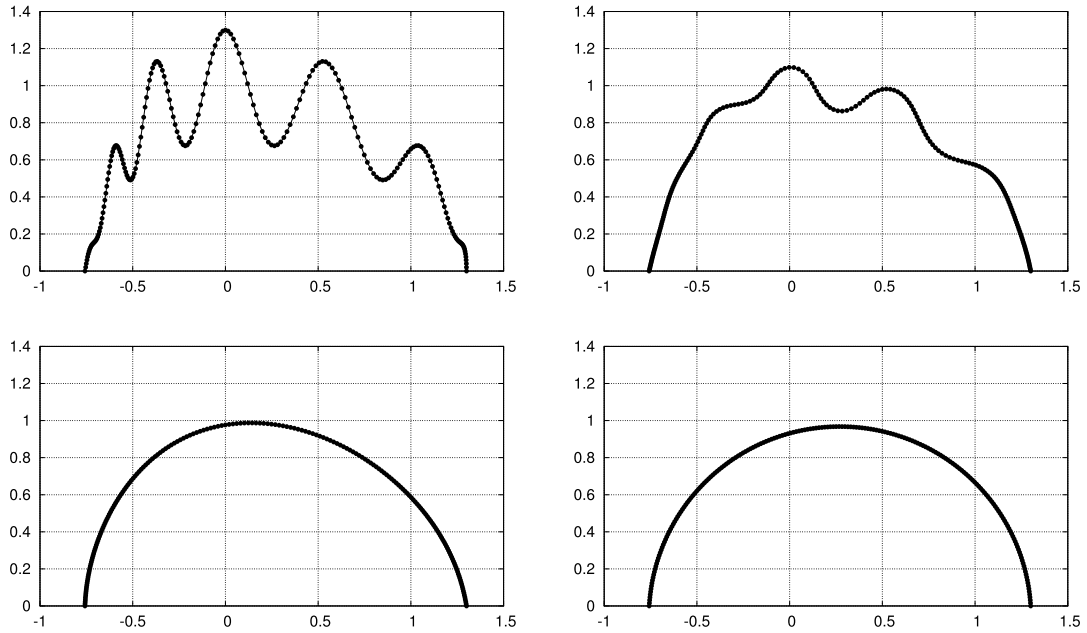


Fig. 5. The area-preserving (mean) curvature flow (1) from Example 2, where the initial open curve asymptotically approaches the arc shape. The curve Γ_t is depicted for $t = 0, t = 0.0125, t = 0.1$ and $t = 2.0$.

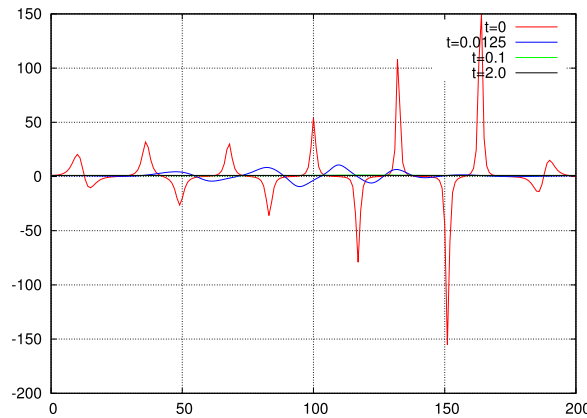


Fig. 6. Time evolution of the curvature from Example 2 for $M = 200$ finite volumes.

is just the area below the graph of the curve. As seen in Fig. 6, the initial curve exhibits high variation of curvature, whereas the curvature of steady state remains constant. The initial curve encloses the area of 1.53819 and at $t = 2.0$, the curve encloses the area of 1.53866. Table 1 shows the values of EoC for enclosed area.

Example 3. In Fig. 7, the third example shows the behavior of the solution when the initial open curve is given by parametric equations

$$\vec{X}(0, u) = \left((0.75 + 0.25 \cos(4\pi u)) \cos(\pi u), (0.5 + \cos(5\pi u)) \sin(\pi u) \right) \tag{27}$$

for $u \in [0, 1]$. The motion in the time interval $[0, 5.0]$ is driven by the normal velocity given by (1). The number of finite volumes is $M = 200$. The curve Γ_t asymptotically approaches the arc shape, where the preserved quantity A_t is just the area below the graph of the curve. As seen in Fig. 8, the initial curve exhibits high variation of curvature, whereas the curvature of steady state remains constant. The initial curve encloses the area of 0.58902 and at $t = 5.0$, the curve encloses the area of 0.58926. Table 1 shows the values of EoC for enclosed area.

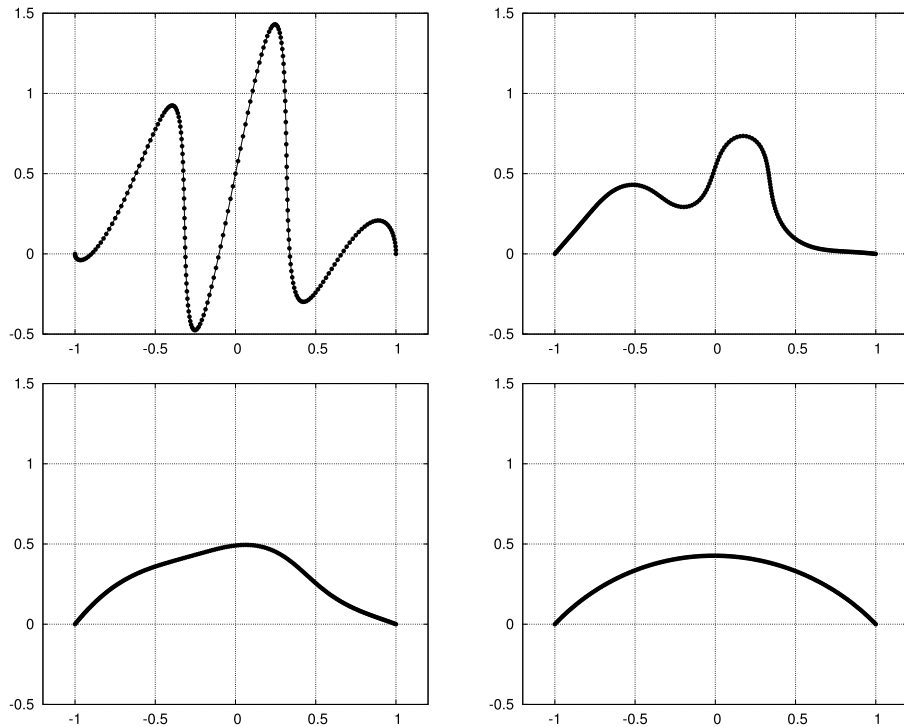


Fig. 7. The area-preserving (mean) curvature flow (1) from Example 3, where the initial open curve asymptotically approaches the arc shape. The curve Γ_t is depicted for $t = 0, t = 0.05, t = 0.1$ and $t = 5.0$.

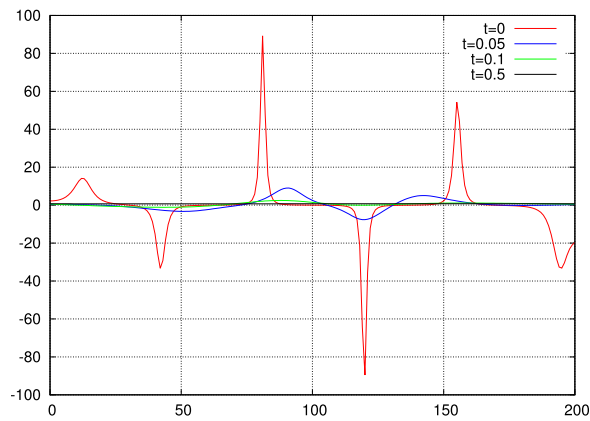


Fig. 8. Time evolution of the curvature from Example 3 for $M = 200$ finite volumes.

Example 4. In Fig. 9, the fourth example shows the behavior of the solution when the initial open curve is given by parametric equations

$$\vec{X}(0, u) = \left((0.75 + 0.25 \cos(5\pi u) + 0.25 \sin(5\pi u)) \cos(\pi u), (0.5 + 0.5 \cos(5\pi u) + 0.5 \sin(5\pi u)) \sin(\pi u) \right) \tag{28}$$

for $u \in [0, 1]$. The motion in the time interval $[0, 2.0]$ is driven by the normal velocity given by (1). The number of finite volumes is $M = 200$. The curve Γ_t asymptotically approaches the arc shape, where the preserved quantity A_t is just the area below the graph of the curve. The initial curve encloses the area of 0.825874 and at $t = 2.0$, the curve encloses the area of 0.824312069605. Table 1 shows the values of EoC for enclosed area.

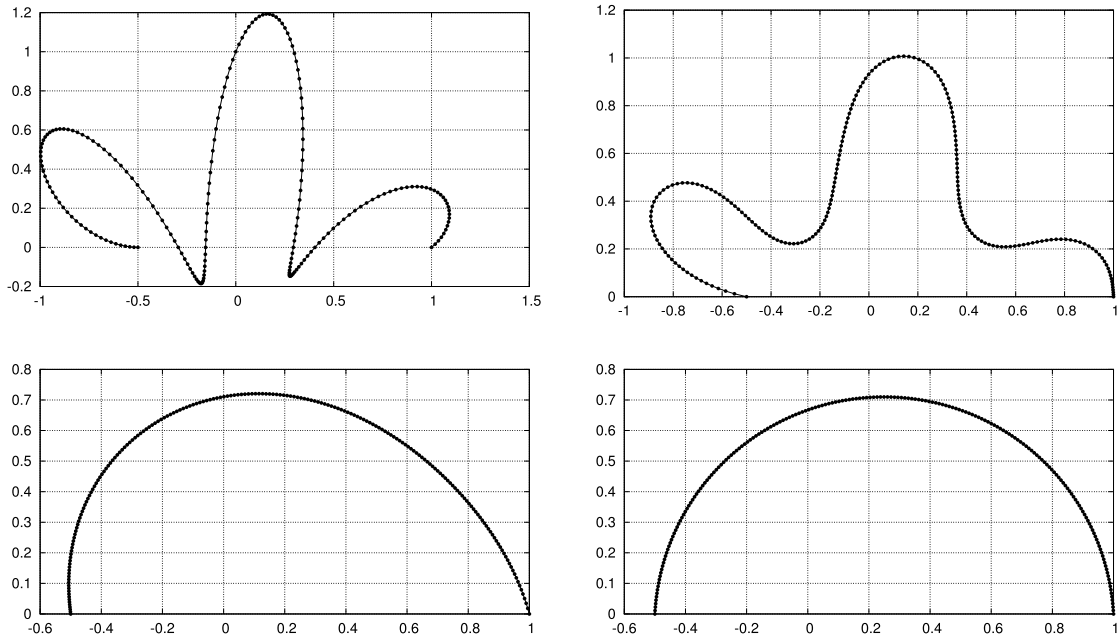


Fig. 9. The area-preserving (mean) curvature flow (1) from Example 4, where the initial open curve asymptotically approaches the arc shape. The curve Γ_t is depicted for $t = 0$, $t = 0.025$, $t = 0.2$ and $t = 2.0$.

Table 1
Table of EoC for Examples 1–5.

	M	$error_1$ (EoC for $error_1$)	EoC	$error_2$ (EoC for $error_2$)	EoC
Example 1 $A(\Gamma_{ini}) = 0.533269$	100	0.000017583819	–	0.000019645546	–
	200	0.000008454447	1.056	0.000008761386	1.165
	300	0.000004374383	1.625	0.000004492787	1.647
	400	0.000002643685	1.751	0.000002706492	1.762
	500	0.000001765270	1.810	0.000001804284	1.817
Example 2 $A(\Gamma_{ini}) = 1.53819$	100	0.009968971070	–	0.009933596328	–
	200	0.000499490704	4.319	0.000498814330	4.316
	300	0.000183365980	2.471	0.000183093782	2.472
	400	0.000100446450	2.092	0.000100287455	2.092
Example 3 $A(\Gamma_{ini}) = 0.58902$	500	0.000064864539	1.960	0.000064757573	1.960
	100	0.006099061574	–	0.005900274464	–
	200	0.000216169514	4.818	0.000200691023	4.878
	300	0.000102164881	1.848	0.000094836643	1.849
	400	0.000058271550	1.952	0.000054052171	1.954
Example 4 $A(\Gamma_{ini}) = 0.825874$	500	0.000037510079	1.974	0.000034774945	1.977
	100	0.005547674900	–	0.005385431344	–
	200	0.001561930395	1.829	0.001511765019	1.833
	300	0.000730291865	1.875	0.000707040287	1.874
	400	0.000420150011	1.922	0.000406979651	1.920
Example 5 $A(\Gamma_{ini}) = 0.651942$	500	0.000271559188	1.956	0.000263163652	1.954
	100	0.002450053055	–	0.002438076928	–
	200	0.000713227097	1.780	0.000710694296	1.778
	300	0.000342511990	1.809	0.000341409141	1.808
	400	0.000196973384	1.923	0.000196359571	1.923
500	0.000126204707	1.995	0.000125817158	1.995	

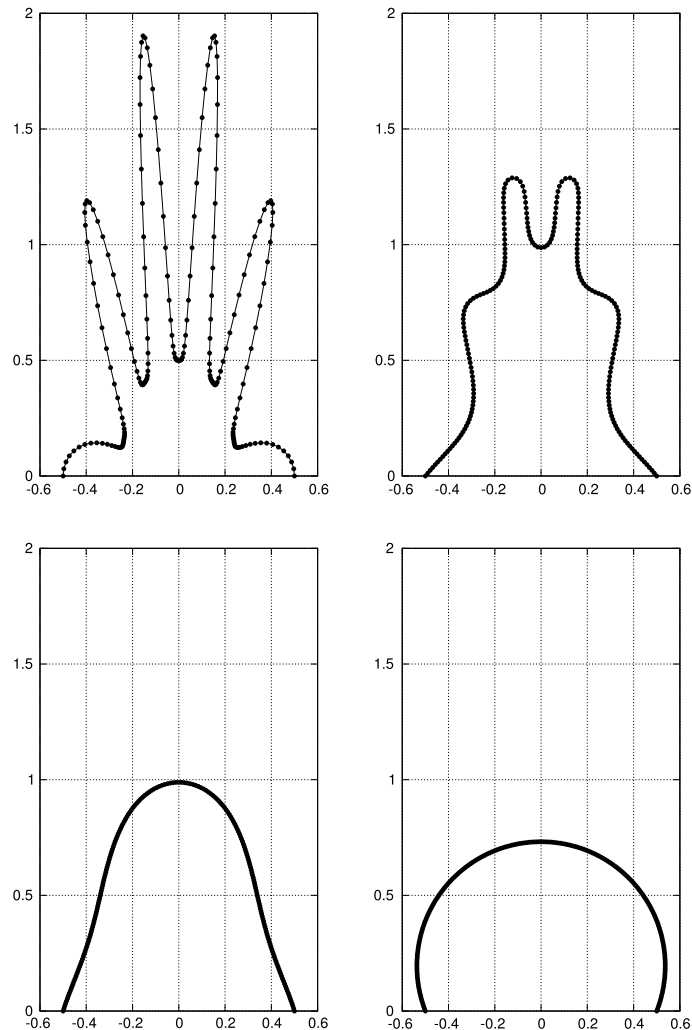


Fig. 10. The area-preserving (mean) curvature flow (1) from Example 5, where the initial open curve asymptotically approaches the arc shape. The curve Γ_t is depicted for $t = 0$, $t = 0.0125$, $t = 0.05$ and $t = 2.0$.

Example 5. In Fig. 10, the fifth example shows the behavior of the solution when the initial open curve is given by parametric equations

$$\vec{X}(0, u) = \left((0.25 + 0.25 \cos^4(5\pi u)) \cos(\pi u), (0.5 + 1.5 \cos^4(5\pi u)) \sin(\pi u) \right) \quad (29)$$

for $u \in [0, 1]$. The motion in the time interval $[0, 2.0]$ is driven by the normal velocity given by (1). The number of finite volumes is $M = 200$. The curve Γ_t asymptotically approaches the arc shape, where the preserved quantity A_t is just the area below the graph of the curve. The initial curve encloses the area of 0.651942 and at $t = 2.0$, the curve encloses the area of 0.652655227097. Table 1 shows the values of EoC for enclosed area.

5. Conclusion

In this paper we analyzed the area-preserving (mean) curvature flow of open curves and its qualitative and quantitative behavior of solutions obtained numerically by means of the flowing finite volumes method. Our computations confirmed the hypothesis that the solution attains an arc shape in long-term. This behavior corresponds to the expected use in modeling the recrystallization phenomena in solid phase.

Acknowledgments

The first two authors were partly supported by the project No. 14-36566G “*Multidisciplinary research centre for advanced materials*” of the Grant Agency of the Czech Republic. The third author was supported by the VEGA grant 1/0780/15 (DS).

References

- [1] S. Allen, J. Cahn, A microscopic theory for antiphase boundary motion and its application to antiphase domain coarsening, *Acta Metall.* 27 (1979) 1084–1095.
- [2] M. Beneš, Diffuse-interface treatment of the anisotropic mean-curvature flow, *Appl. Math.* 48 (6) (2003) 437–453.
- [3] M. Beneš, V. Chaloupecký, K. Mikula, Geometrical image segmentation by the Allen–Cahn equation, *Appl. Numer. Math.* 51 (2004) 187–205.
- [4] M. Beneš, M. Kimura, P. Pauš, D. Ševčovič, T. Tsujikawa, S. Yazaki, Application of a curvature adjusted method in image segmentation, *Bull. Inst. Math. Acad. Sin. (N.S.)* 3 (2008) 509–523.
- [5] M. Beneš, J. Kratochvíl, J. Kříšť'an, V. Minárik, P. Pauš, A parametric simulation method for discrete dislocation dynamics, *Eur. Phys. J. ST* 177 (2009) 171–191.
- [6] M. Beneš, J. Kratochvíl, J. Kříšť'an, V. Minárik, P. Pauš, A parametric simulation method for discrete dislocation dynamics, *Eur. Phys. J. ST* 177 (2009) 177–192.
- [7] M. Beneš, S. Yazaki, M. Kimura, Computational studies of non-local anisotropic Allen–Cahn equation, *Math. Bohem.* 136 (4) (2011) 429–437.
- [8] J.W. Cahn, J.E. Hilliard, Free energy of a nonuniform system, III. Nucleation of a two-component incompressible fluid, *J. Chem. Phys.* 31 (1959) 688–699.
- [9] K. Deckelnick, Parametric mean curvature evolution with a dirichlet boundary condition, *J. Reine Angew. Math.* 459 (1995) 37–60.
- [10] K. Deckelnick, Weak solutions of the curve shortening flow, *Calc. Var. Partial Differential Equations* 5 (1997) 489–510.
- [11] I.C. Dolcetta, S.F. Vita, R. March, Area preserving curve shortening flows: from phase separation to image processing, *Interfaces Free Bound.* 4 (2002) 325–343.
- [12] G. Dziuk, K. Deckelnick, C.M. Elliott, Computation of geometric partial differential equations and mean curvature flow, *Acta Numer.* 14 (2005) 139–232.
- [13] S. Esedoğlu, S. Ruuth, R. Tsai, Threshold dynamics for high order geometric motions, *Interfaces Free Bound.* 10 (3) (2008) 263–282.
- [14] M. Gage, On an area-preserving evolution equation for plane curves, *Contemp. Math.* 51 (1986) 51–62.
- [15] M. Gage, R. Hamilton, The heat equation shrinking convex plane curves, *J. Differential Geom.* 23 (1986) 285–314.
- [16] M. Grayson, The heat equation shrinks embedded plane curves to round points, *J. Differential Geom.* 26 (1987) 285–314.
- [17] M. Henry, D. Hilhorst, M. Mimura, A reaction–diffusion approximation to an area preserving mean curvature flow coupled with a bulk equation, *Discrete Contin. Dyn. Syst. Ser. S* 4 (1) (2011) 125–154.
- [18] C. Kublik, S. Esedoğlu, J.A. Fessler, Algorithms for area preserving flows, *SIAM J. Sci. Comput.* 33 (2011) 2382–2401.
- [19] I.V. Markov, *Crystal Growth for Beginners: Fundamentals of Nucleation, Crystal Growth, and Epitaxy*, second ed., World Scientific Publishing Company, 2004.
- [20] J. McCoy, The surface area preserving mean curvature flow, *Asian J. Math.* 7 (1) (2003) 7–30.
- [21] K. Mikula, D. Ševčovič, Computational and qualitative aspects of evolution of curves driven by curvature and external force, *Comput. Vis. Sci.* 6 (2004) 211–225.
- [22] V. Minárik, M. Beneš, J. Kratochvíl, Simulation of dynamical interaction between dislocations and dipolar loops, *J. Appl. Phys.* 107 (2010) 061802.
- [23] L. Osaki, H. Satoh, S. Yazaki, Towards modelling spiral motion of open plane curves, *Discrete Contin. Dyn. Syst. Ser. S* 8 (5) (2015) 1009–1022.
- [24] S. Osher, J. Sethian, Fronts propagating with curvature dependent speed: Algorithms based on Hamilton–Jacobi formulations, *J. Comput. Phys.* 79 (1988) 12–49.
- [25] P. Pauš, J. Kratochvíl, M. Beneš, A dislocation dynamics analysis of the critical cross-slip annihilation distance and the cyclic saturation stress in fcc single crystals at different temperatures, *Acta Mater.* 61 (2013) 7917–7923.
- [26] P. Pauš, J. Kratochvíl, M. Beneš, Mechanisms controlling the cyclic saturation stress and the critical cross-slip annihilation distance in copper single crystals, *Phil. Mag. Lett.* 94 (2014) 45–52.
- [27] J. Rubinstein, P. Sternberg, Nonlocal reaction–diffusion equations and nucleation, *IMA J. Appl. Math.* 48 (1992) 249–264.
- [28] D. Ševčovič, Qualitative and quantitative aspects of curvature driven flows of planar curves, in: P. Kaplický, Š. Nečasová (Eds.), *Topics on Partial Differential Equations*, Jindřich Nečas Center for Mathematical Modeling Lecture Notes, Vol. 2, Prague, pp. 55–119.
- [29] D. Ševčovič, K. Mikula, Evolution of plane curves driven by a nonlinear function of curvature and anisotropy, *SIAM J. Appl. Math.* 61 (2001) 1473–1501.
- [30] D. Ševčovič, S. Yazaki, On a gradient flow of plane curves minimizing the anisoperimetric ratio, *IAENG Int. J. Appl. Math.* 43 (2013) 160–171.